Improving the responses of the Australian community land surface model (CABLE) to seasonal drought

Longhui Li,[1] Ying-Ping Wang,[2] Qiang Yu,[1] Bernard Pak,[2] Derek Eamus,[1] Junhua Yan,[3] Eva van Gorsel,[4] and Ian T. Baker[5]

Received 27 March 2012; revised 14 August 2012; accepted 15 August 2012; published 11 October 2012.

[1] Correct representations of root functioning, such as root water uptake and hydraulic redistribution, are critically important for modeling the responses of vegetation to droughts and seasonal changes in soil moisture content. However, these processes are poorly represented in global land surface models. In this study, we incorporated two root functions: a root water uptake function which assumes root water uptake efficiency varies with rooting depth, and a hydraulic redistribution function into a global land surface model, CABLE. The water uptake function developed by Lai and Katul (2000) was also compared with the default one (see Wang et al., 2010) that assumes that efficiency of water uptake per unit root length is constant. Using eddy flux measurements of CO_2 and water vapor fluxes at three sites experiencing different patterns of seasonal changes in soil water content, we showed that the two root functions significantly improved the agreement between the simulated fluxes of net ecosystem exchange and latent heat flux and soil moisture dynamics with those observed during the dry season while having little impact on the model simulation during the wet seasons at all three sites. Sensitivity analysis showed that varying several model parameters influencing soil water dynamics in CABLE did not significantly affect the model's performance. We conclude that these root functions represent a valuable improvement for land surface modeling and should be implemented into CABLE and other land surface models for studying carbon and water dynamics where rainfall varies seasonally or interannually.

Citation: Li, L., Y.-P. Wang, Q. Yu, B. Pak, D. Eamus, J. Yan, E. van Gorsel, and I. T. Baker (2012), Improving the responses of the Australian community land surface model (CABLE) to seasonal drought, *J. Geophys. Res.*, *117*, G04002, doi:10.1029/2012JG002038.

1. Introduction

[2] Land surface models (LSMs), as a key component of global circulation models (GCMs) for regional or global climate projections, provide the lower boundary conditions of GCMs, i.e., control the amount of available energy and its partitioning between sensible and latent heat fluxes [*Shukla and Mintz*, 1982; *Mintz*, 1984]. The latent heat flux from a land surface depends on atmospheric demand [*Jarvis and McNaughton*, 1986], the supply of soil water through plant roots [*Cowan*, 1965; *Tuzet et al.*, 2003] and several characteristics of vegetation, including root depth and leaf area index. Under well watered conditions, the performance of several global land surface models, including the Australian community land surface model (CABLE) perform reasonably well [see *Krinner et al.*, 2005; *Wang et al.*, 2010; *Bonan et al.*, 2011]. When soil water availability is limiting, however, the performance of such models is poor [see *Abramowitz et al.*, 2007]. For example, recent studies have found that several global models predict Amazonian tropical evergreen broadleaf forests to be a carbon sink during the wet season and a carbon source during the dry season [*Raich et al.*, 1991; *Potter et al.*, 2001]. Observational evidence, however, shows that the actual carbon dynamics are more heterogeneous, with different sites behaving as sources and sinks at different times according to the seasonality of rainfall. Sites with little seasonality [*Araújo et al.*, 2002; *Carswell et al.*, 2002] show less within-year variability in C and water fluxes while sites with a strong seasonality in rainfall in the Amazon can be a carbon sink during the dry season and source during rainy periods [*Saleska et al.*, 2003]. A study on another site in the Amazon found that the forest was a sink during the rainy season and a source

[1]Plant Functional Biology and Climate Change Cluster, University of Technology, Sydney, New South Wales, Australia.
[2]CSIRO Marine and Atmosphere Division, Aspendale, Victoria, Australia.
[3]South China Botanic Garden, Chinese Academy of Sciences, Guangzhou, China.
[4]CSIRO Marine and Atmospheric Research, Canberra, ACT, Australia.
[5]Department of Atmospheric Science, Colorado State University, Fort Collins, Colorado, USA.

Corresponding author: L. Li, Plant Functional Biology and Climate Change Cluster, University of Technology, PO Box 123, Sydney, NSW 2007, Australia. (Longhui.Li@uts.edu.au)

0148-0227/12/2012JG002038

during dry season [*Vourlitis et al.*, 2001]. Because net ecosystem carbon exchange is a small difference between two large carbon fluxes: gross primary production (GPP) and total ecosystem respiration (TER). A small change in either GPP or TER can have quite large influences on NEE.

[3] During dry seasons of wet-dry regions (for example, African and Australian savannas), many tree species do not suffer from significant water stress as a result of one or several adaptive mechanisms: such as a dry season deciduous habit, deep rooting and/or a large capacity for osmoregulation [*Eamus and Prior*, 2001]. Under a given climate condition, whether plants will suffer from severe water stress during the dry seasons critically depends on rooting depth, the ability of roots to take up water from deep moist soil, and hydraulic redistribution (the ability to redistribute water from wet to dry parts of the profile [see *Jackson et al.*, 2000]). Plant root systems show great plasticity in rooting depth and root-density distribution as a function of soil water and nutrient contents [*Feddes et al.*, 2001]. In arid and semiarid regions, plants can have active roots at a soil depth >30 m [*Canadell et al.*, 1996] and these deeper roots can take up more water than surface roots [*Pate et al.*, 1995; *Jackson et al.*, 2000; *McElrone et al.*, 2004]. Water can also move passively from moist to dry portions of the soil through roots in the process of hydraulic redistribution (HR) [*Caldwell et al.*, 1998; *Burgess et al.*, 1998; *Burgess et al.*, 2001; *Bleby et al.*, 2010]. During dry periods, hydraulic redistribution allows water to move overnight from deep moist soil to the dry surface soil layer where plant roots are more abundant. Consequently transpiration is sustained [*Richards and Caldwell*, 1987]. During wet periods, water can also move down from the surface layer to deep layer via roots to minimize loss through surface runoff [*Burgess et al.*, 1998] or evaporation. Hydraulic redistribution has been demonstrated for many plant species, including tropical and subtropical forests [*Caldwell et al.*, 1998; *Burgess et al.*, 1998; *Oliveira et al.*, 2005; *Bleby et al.*, 2010]. These mechanisms can all exert a strong influence on stomatal conductance, latent heat flux and energy partitioning, especially during the dry seasons [*Lee et al.*, 2005; *Zheng and Wang*, 2007; *Baker et al.*, 2008].

[4] Despite extensive documentation globally, few of these processes have been incorporated into most global LSMs [*Lee et al.*, 2005; *Baker et al.*, 2008]. Most LSMs represent root-water uptake as a sink term in the Richards equation [*Feddes et al.*, 2001], and root-water uptake is commonly modeled as a function of atmospheric demand and root density distribution within the soil (for example, SiB [*Sellers et al.*, 1996; *Denning et al.*, 1996], CLM (Community Land Model) [*Dai et al.*, 2003; *Oleson et al.*, 2004] and CABLE [*Kowalczyk et al.*, 2006; *Wang et al.*, 2010]). Rooting depth is often fixed in most land surface models for the sake of numerical efficiency, with the exception of SiB3, which was recently modified to have roots down to 10 m [*Baker et al.*, 2008] in the soil of tropical forests. Similarly, variation of water uptake per unit root mass at different soil depths is not accounted for in most LSMs [*Lai and Katul*, 2000]. Hydraulic redistribution was only recently tested in CLM [see *Lee et al.*, 2005] or SiB3 [see *Baker et al.*, 2008] at one site, or has yet to be implemented into other LSMs.

[5] One of most contentious issues in global change research is the projected significant loss of Amazon forest in response to drier climate conditions in the future [*Cook and Vizy*, 2008; *Huntingford et al.*, 2008; *Jones et al.*, 2009]. Observations from in situ and remote sensing did not show significant decreases in canopy transpiration and photosynthesis from wet to dry seasons in the Amazonia tropical rain forests [*Saleska et al.*, 2003; *Saleska et al.*, 2007]. Several global land models can't correctly reproduce this response of tropical forests to seasonal drought [*Saleska et al.*, 2003], including SiB, unless contribution to plant water use by deep soil water uptake or hydraulic redistribution are accounted for, as demonstrated by *Baker et al.* [2008]. Even for simple paradigmatic hydrological models, a contribution of deep soil moisture to evapotranspiration should be taken into account [*Thompson et al.*, 2011]. Without consideration of these root functions in GCMs, latent heat flux may be considerably underestimated, and hence the surface climate cannot accurately be simulated by GCMs [*Kleidon and Heimann*, 2000].

[6] In this study, we use CABLE to study the effects of two root functions on the simulated responses of net ecosystem carbon exchange (NEE) and latent heat flux (Q_{LE}) to dry season conditions. The first function describes water uptake at depth; the second is a hydraulic redistribution function. We compare these simulations with in situ measurements from three evergreen broadleaf forests in temperate, subtropical and tropical climates. These three forests were chosen because they are represented in CABLE as the same plant functional type and consequently they have all the same model parameter values except for canopy leaf area index. More importantly, they have very different annual totals for rainfall and their seasonal distribution of rainfall also differ. We did not modify rooting depth in CABLE, as this would reduce computing efficiency when CABLE is applied globally. The objectives of this study were (1) to quantify the effects of two different functions for water uptake by roots or hydraulic redistribution or both on the simulated soil water dynamics and NEE and Q_{LE} for the three forests; (2) to compare the simulated NEE, Q_{LE} and soil water content with in situ observations at both daily and seasonal timescales; (3) to determine how the effects of root water uptake function and hydraulic redistribution vary with other key model parameters for the simulated soil water dynamics in a forest ecosystem by CABLE; and hence (4) to investigate if tuning parameters are able to improve CABLE's performance and finalize the essentiality of root functioning to CABLE.

2. Methods

2.1. Description of the Sites and Measurements

[7] Three evergreen broadleaf forests from temperate, subtropical and tropical climates were selected for this study. All three forests are considered as the same plant functional type in CABLE, but have different total annual rainfall and seasonal distribution of rainfall.

[8] The temperate forest site, Tumbarumba (AU-Tum) is located in southeast Australia (35.66°S, 148.15°E). The dominant species in the upper canopy is *Eucalyptus delegatensis* and *E. dalrympleana* while the patchy understorey consists of shrubs and grasses. Mean height of the

overstorey canopy is 40 m. Total canopy leaf area index (LAI) varied between 2.3 and 3.5 [see *Wang et al.*, 2011], with a marked seasonal variation. Climate is Mediterranean with a hot and dry summer and wet and cool winters. Mean annual rainfall is 896 mm, mean annual air temperature of 9.3°C over the study period from 2002 to 2006. The dry season is from October to March, with about 34% of annual rainfall received in these 6 months. Over the study period, the forest experienced severe drought in 2003 and 2006 [see *Keith et al.*, 2009, 2011, for further details].

[9] The subtropical forest site, Dinghushan (CN-Dhs) is located in south China (23.17°N, 112.53°E). The dominant species include *Schima superb* and *Castanopisis chinensis* in the upper canopy layer and *Cryptocarya concinna* and *Machilus chinensis* in the lower canopy layer. The mean height of the upper canopy layer is about 17 m. Total LAI of the forest is about 5, and remains relatively constant throughout the year [*Wang et al.*, 2006; *M. Zhang et al.*, 2011; *Tang et al.*, 2011]. Climate is strongly influenced by subtropical monsoon with distinct wet and dry seasons. The mean annul air temperature is 20.4°C, mean annual solar radiation 140 W m^{-2}, and the mean annual rainfall is 1337 mm with only 10% of annual rainfall occurring during the dry season (October–March) over the study period 2003–2005.

[10] The tropical forest site, Tapajos National Forest km83 (BR-Sa3) is located within the Tapajos National Forest, Pará, Brazil (3.02°S, 54.97°W). Dominant tree species include *Couratari guianensis*, *Eschweilera* spp., *Manilkara huberi*, *Carapa guianensis*, *Sclerolobium paniculatum*, *Pouteria* spp., *Protium decandro*, and *Licaria guianensis* [*Negrón Juárez et al.*, 2009]. Average height of the overstorey canopy is about 35 m. The total LAI varies between 4.1 and 5.1, as estimated from MODIS measurements (LBA-MIP protocol, http://www.climatemodeling.org/lba_mip/lba_mip_protocol4.0_20100309.pdf). During the study period 2001–2003, the mean annual air temperature and solar radiation were 25.9°C and 185.6 W m^{-2}, respectively. The mean annual total rainfall was 1659 mm with only 24% of rainfall occurring in the dry season from July to December from 2001 to 2003.

[11] At each site an eddy covariance (EC) system was installed to measure the fluxes of CO_2 and latent heat and all meteorological variables required for running the CABLE model. Eddy flux measurements from each site over the study periods here have been used previously, and more information is provided in *Keith et al.* [2009, 2011] and *van Gorsel et al.* [2007] for the AU-Tum site, *M. Zhang et al.* [2011] for the CN-Dhs site, and *Goulden et al.* [2004] and *Miller et al.* [2004] for the BR-Sa3 site. Estimates of monthly GPP and TER were provided by researchers from each site, except for the BR-Sa3 where monthly mean GPP and TER were digitized from a figure in *Saleska et al.* [2003, Figure 2b]. At the AU-Tum site, hourly GPP was calculated as the difference between hourly NEE and hourly TER. The latter was calculated using a temperature response function derived from nighttime respiration and soil temperatures [*van Gorsel et al.*, 2008]. These estimates agree to within the 95% confidence level with respiration estimates derived from an NEE light response curve [*van Gorsel et al.*, 2009]. At the CN-Dhs site, NEE was partitioned into GPP and TER using the method described by *Reichstein et al.* [2005]. Further details on flux partitioning and data quality check can be found in *Yu et al.* [2006]. At the BR-Sa3 site, digitized monthly mean GPP is calculated based on half-hourly values of TER-NEE. Half-hourly TER equals NEE at night and is assumed to have the same average value during the day as at night [*Saleska et al.*, 2003].

[12] For AU-Tum, canopy LAI varies monthly and their values are taken from *Wang et al.* [2011]. At the CN-Dhs site, the canopy LAI is 5 [see *Wang et al.*, 2006]. Continuous measurements of soil moisture at different depths are available at the AU-Tum and BR-Sa3 sites. At the AU-Tum site, hourly soil moisture at depths of 0–15 cm, 15–30 cm, 30–60 cm and 60–120 cm was measured using time domain reflectometry (TDR) [*Zegelin and White*, 1989]. These data were previously used by *Keith et al.* [2009]. At the BR-Sa3 site, hourly soil moisture at 10 different depths from 15 cm to 1000 cm was measured at 10 different depths from 15 cm to 1000 cm (http://daac.ornl.gov/citation_policy.html), but only measurements from 15 cm to 400 cm were used for comparison here because the total soil depth as represented in CABEL is 460 cm.

2.2. Model Description

[13] The Community Atmosphere-Biosphere Land Exchange, CABLE, is a global land surface model that simulates exchange of momentum, energy, water and CO_2 between the lower atmosphere and land surface [see *Kowalczyk et al.*, 2006; *Wang et al.*, 2010]. CABLE has been evaluated against eddy flux measurements from a range of ecosystems and its performance is comparable to other global land surface models [*Abramowitz et al.*, 2007; *Wang et al.*, 2007]. It has also been used to study systematic model errors [*Abramowitz*, 2005; *Wang et al.*, 2010], effects of land cover change on regional climate [*Cruz et al.*, 2010; *Pitman et al.*, 2011], and regional water balances [*H. Q. Zhang et al.*, 2011].

[14] A detailed description of CABLE can be found in *Kowalczyk et al.* [2006] and *Wang et al.* [2010], only some parts related to the present study are described here. In CABLE, the total latent heat flux (λE) is the sum of the latent heat fluxes from the canopy (both dry and wet parts) and the soil. That is,

$$\lambda E = (1 - f_{wet})\lambda E_{dry} + f_{wet}\lambda E_{wet} + \lambda E_s, \quad (1)$$

where λ is the latent heat of vaporization (J kg^{-1}), λE_{dry}, λE_{wet}, and λE_s are the latent heat fluxes of dry, wet canopy, and soil in W m^{-2}. The canopy wet fraction, f_{wet}, is calculated as a function of canopy water [see *Wang et al.*, 2010].

2.2.1. Two Root Water Extraction Functions

[15] Canopy transpiration rate from a dry canopy, E_{dry}, is calculated as

$$E_{dry} = \sum_{i=1}^{n} \min\left((1 - f_{wet})\eta_i E^*_{dry}, 1000(\theta_i - \theta_{wilt})\Delta z/\Delta t\right), \quad (2)$$

where Δz is the thickness of soil layer i in m, and Δt is the time step of CABLE (1800 s or 3600 s in this study), the factor 1000 is for converting soil depth from m to mm. θ_i and θ_{wilt} are soil moisture content and wilting point, respectively. E^*_{dry} is the canopy transpiration rate when the rate of soil water supply is not limiting, and is calculated with the stomatal conductance estimated using equation (A18) of *Wang et al.* [2010] for sunlit and shaded leaves separately. η_i is the

fraction of dry canopy transpiration ($(1 - f_{wet})\ E^*_{dry}$) extracted from soil layer *i*.

[16] Two methods are compared for estimating η_i. In the default version of CABLE, η_i is calculated as

$$\eta_i = \frac{f_{root,i}\frac{\theta_i - \theta_{wilt}}{\theta_{sat} - \theta_{wilt}}}{\sum_{i=1}^{n} f_{root,i}\frac{\theta_i - \theta_{wilt}}{\theta_{sat} - \theta_{wilt}}}, \quad (3)$$

where θ_{sat} is the saturated soil moisture content, and $f_{root,i}$ is the fraction of root mass in soil layer *i* and is calculated by a formula proposed by *Jackson et al.* [1996].

[17] The alternative model for computing η_i is based on the root water uptake function developed by *Lai and Katul* [2000]. That is

$$\eta_i = \frac{f_{root,i}\alpha_{i,1}\alpha_{i,2}}{\sum_{i=1}^{n} f_{root,i}\alpha_{i,1}\alpha_{i,2}}, \quad (4)$$

where

$$\alpha_{i,1} = \max\left\{\frac{\theta_i}{\theta_{sat} - \theta_{wilt}}, \frac{\int_{i=1}^{i}\theta_i dz}{\int_{i=1}^{n}\theta_i dz}\right\}, \quad (5)$$

$$\alpha_{i,2} = \left(\frac{\theta_i - \theta_{wilt}}{\theta_{sat}}\right)^{\gamma/\theta_i - \theta_{wilt}}, \quad (6)$$

where γ is an empirical constant, and is equal to 0.01 in this study [see *Lai and Katul*, 2000], z is soil layer depth. Equation (4) must satisfy the constraint $\int_{i=1}^{n}\alpha_{i,1}\alpha_{i,2}dz \le 1$.

[18] In equation (4), $\alpha_{i,1}$ represents a maximal efficiency of water uptake by roots when root water uptake is not limited by available soil water (or $\alpha_{i,2} = 1$) and $\alpha_{i,2}$ represents the decrease in root uptake efficiency with soil water, and is equal to zero when the soil water in the layer is equal to wilting point.

2.2.2. Hydraulic Redistribution

[19] Soil is divided into six layer in CABLE, and thickness of the six layers from the top to bottom are 2.2 cm, 5.8 cm, 40.9 cm, 108.5 cm, 287.2 cm. Change in soil water within each layer was modeled using the θ-based Richards equation based on the Buckingham-Darcy law. That is:

$$\frac{\partial\theta}{\partial t} = -\frac{\partial q}{\partial z} - E_x + H, \quad (7)$$

where q is the kinematic moisture flux (m s^{-1}, and positive for flux downward), E_x is the water lost from soil due to soil evaporation or root extraction (m s^{-1}) ($E_x = E_{dry} + E_s$), and H is the net water flux from hydraulic redistribution (m s^{-1}).

[20] The kinematic moisture flux, q, is simulated using the Darcy' law. That is

$$q = -D\frac{\partial\theta}{\partial z} + K, \quad (8)$$

where K is hydraulic conductivity (m s^{-1}), D is soil moisture diffusivity (m^2 s^{-1}) and is calculated as $\frac{K\partial\psi}{\partial\theta}$ where ψ is soil matrix potential in m. The relationship between K or ψ and θ are described using the equations of *van Genuchten* [1980]. They are

$$K = K_{sat}\sqrt{\frac{\theta_i - \theta_r}{\theta_{sat} - \theta_r}}\left(1 - \left(1 - \left(\frac{\theta_i - \theta_r}{\theta_{sat} - \theta_r}\right)^{\frac{\upsilon}{\upsilon-1}}\right)^{\frac{\upsilon-1}{\upsilon}}\right)^2, \quad (9)$$

$$\psi = -\frac{1}{a}\left(\left(\frac{\theta_i - \theta_r}{\theta_{sat} - \theta_r}\right)^{\frac{\upsilon}{\upsilon-1}} - 1\right)^{\frac{1}{\upsilon}}, \quad (10)$$

where K_{sat}, ψ_{sat} are the hydraulic conductivity and soil matrix potential at saturation, respectively; θ_r is the residual and saturated volumetric water contents (m^3 m^{-3}). υ and a are empirical parameters that vary with soil texture. Equation (7) can be integrated numerically with the following boundary conditions:

$$q = P - E_s \text{ at } z = 0, \quad (11)$$

$$q = c_d\theta \text{ at } z = Z, \quad (12)$$

where P is precipitation (m s^{-1}), c_d is soil drainage coefficient and Z is the depth of the bottom soil layer (m). See *Kowalczyk et al.* [2006] for further details.

[21] Water flux between different soil layers from hydraulic redistribution, H, is calculated based on two main constraints: the root density and the rhizosphere conductivity of the supplying layer. Following *Ryel et al.* [2002], H_i from one soil layer is calculated as

$$H_i = C_{RT}\sum_{i=1}^{n}(\psi_i - \psi_j)\max(c_i, c_j)\frac{f_{root,i}f_{root,j}}{1 - f_{root,X}}\delta_T, \quad (13)$$

where C_{RT} is the maximum radial soil-root conductance of the entire active root system for water (m MPa^{-1} s^{-1}), ψ_i is soil water potential (m) in soil layer i, c_i is a factor representing the effect of soil water potential on soil-root conductance [see *Ryel et al.*, 2002, equation (7)], δ_T is a factor reducing water movement among layers by roots while the plant is transpiring, and is equal to 0 during day time, or 1 during nighttime. $f_{root,X} = f_{root,i}$ when $\theta_i > \theta_j$ or $f_{root,X} = f_{root,j}$ otherwise. Equation (13) will allow soil water to be redistributed vertically, depending on the difference in water potential between the two calculated layers. Layers are numbered as 1 to 6 (top to down soil layers). In this study, we assumed that hydraulic redistribution does not bring water to the first soil layer where water for soil evaporation is extracted, because many superficially shallow roots die in very dry soils [*Ludwig et al.*, 2003; *Ryel et al.*, 2003]. Therefore soil evaporation is not affected by hydraulic redistribution.

[22] The relative soil–root conductance for water, c_i is calculated using an empirical formula [*Ryel et al.*, 2002]

$$c_i = \frac{1}{1 + \left(\frac{\psi_i}{\psi_{50}}\right)^b}. \quad (14)$$

Table 1. Parameters of the Three Study Sites

Site	La Thuile Code	Silt (%)	Clay (%)	Sand (%)	θ_{wilt} ($m^3\ m^{-3}$)	θ_{sat} ($m^3\ m^{-3}$)	θ_r ($m^3\ m^{-3}$)	K_{sat} ($m\ s^{-1}$)	α (m^{-1})	υ —
Tumbarumba	AU-Tum	33	30	37	0.10	0.38	0.08	6.8e-7	0.014	1.403
Dinghushan	CN-Dhs	48	15	37	0.13	0.42	0.05	2.5e-6	0.007	1.582
Tapajos National Forest	BR-Sa3	2	80	18	0.44*	0.60*	0.10	1.7e-6	0.021	1.137

In equation (14), ψ_{50} is the soil water potential (MPa) where conductance is reduced by 50% and b is an empirical parameter.

2.3. Values of Soil Physical Parameters

[23] Values of all model parameters are default values in CABLE for evergreen broadleaf forest [see *Kowalczyk et al.*, 2006] except canopy LAI and soil physical parameters. For the AU-Tum site, values of soil texture, θ_{sat}, and wilting point θ_{wilt} are derived from *McKenzie* [2004]. At the CN-Dhs site, values of soil texture, θ_{sat}, and θ_{wilt} were obtained from the Chinese Ecological Research Network (http://www.cerndata.ac.cn), and at the BR-Sa3 site, soil texture information were taken from LBA-MPI protocol (http://www.climatemodeling.org/lba-mip/lba_mip_protocol4.0_20100309.pdf) and θ_{sat}, and θ_{wilt} were empirically determined as the maximum and minimum observed soil moisture. Three parameters used in hydraulic redistribution model were set to $C_{RT} = 0.097$ cm $MPa^{-1}\ h^{-1}$, b = 3.22, and $\psi_{50} = -1.0$ MPa following *Ryel et al.* [2002]. The parameters for resolving the van Genuchten equation were estimated using the Rosetta model [*Schaap et al.*, 2001] driven from information of soil texture. All soil and hydrological parameter values were listed in Table 1.

2.4. Model Configuration and Sensitive Analysis

[24] Four simulations denoted as S1 to S4 were conducted to assess the effect of two different water uptake functions with or without hydraulic distributions. Default values of all model parameters except those listed in Table 1 are used in all four simulations.

[25] Because of likely strong correlations among model parameters in CABLE, similar performance of a model simulation can be achieved with different combination of model parameter values [see *Wang et al.*, 2001, 2010]. To address this issue, we varied six model parameters within at least ±25% or 0.1/10 times of the values used in S4 (CABLE with both hydraulic redistribution and alternative root water uptake function, our best performing simulation across all three sites); thus a total of twelve additional simulations were conducted for each site. They are denoted S5 to S16 (Table 2).

[26] Six model parameters that were varied for sensitivity study are K_{sat} (saturated hydraulic conductivity), υ (a parameter for calculating soil water potential in the van Genuchten model, equation (10)), ψ_{50} (the soil water potential where conductance is reduced by 50% see equation (14)), γ (an empirical parameter in the *Lai and Katul* [2000] root-water uptake model, see equation (6)), C_{RT} (in equation (13)) and b (in equation (14)).

[27] To further study the implications of the modified CABLE model on global simulations, we conducted two further simulations: one the simulation (S17) used the default values for all vegetation and soil parameters from the parameter look-up tables [see *Kowalczyk et al.*, 2006] and another simulation used the default values as S17 but included Lai and Katul's root water uptake function [*Lai and Katul*, 2000] and hydraulic redistribution model [*Ryel et al.*, 2002] (noted as S18 in Table 2).

2.5. Mathematical Indices for Model's Performance

[28] We used three indices to evaluate the agreement between model simulation and observations. They are: agreement index (d), root mean square error (RMSE), and the correlation coefficient (R) of the linear regression between the observed and simulated fluxes. Following *Willmott* [1981], the agreement index, d is calculated as:

$$d = 1 - \frac{\sum_{j=1}^{N} \left(P_j - Oj\right)^2}{\sum_{j=1}^{N} \left(\left|P_j - \bar{O}\right| + \left|O_j - \bar{O}\right|\right)^2}, \tag{15}$$

where $\bar{O}$ is the mean of observed flux, O_j and P_j are the observed and modeled fluxes at time step j, and N is the total number of observations. d varies between 0 and 1. A value of 1 indicates a perfect match, and 0 indicates no agreement at all.

[29] RMSE is calculated as:

$$\mathrm{RMSE} = \sqrt{\frac{\sum_{j=1}^{N} \left(P_j - O_j\right)^2}{N - 1}}. \tag{16}$$

The smaller the value of RMSE, the better the agreement between the predictions and measurements is.

Table 2. Definitions of Simulations S1–S18

Simulation	Full Name	Reference
S1	Default with described soil and vegetation parameter	*Wang et al.* [2010]
S2	S1+ hydraulic redistribution (HR)	*Ryel et al.* [2002]
S3	S1+ alternative root water uptake	*Lai and Katul* [2000]
S4	S3+ HR	*Ryel et al.* [2002]
S5	S4, 10 K_{sat}	
S6	S4, 0.1 K_{sat}	
S7	S4, 1.25 υ	
S8	S4, 0.75 υ	
S9	S4, 0.75 ψ_{50}	
S10	S4, 1.25 ψ_{50}	
S11	S4, 10 γ	
S12	S4, 0.1 γ	
S13	S4, 1.25 C_{RT}	
S14	S4, 0.75 C_{RT}	
S15	S4, 1.25b	
S16	S4, 0.75b	
S17	Default values used for all soil and vegetation parameters	
S18	S17 + alternative root water uptake + HR	

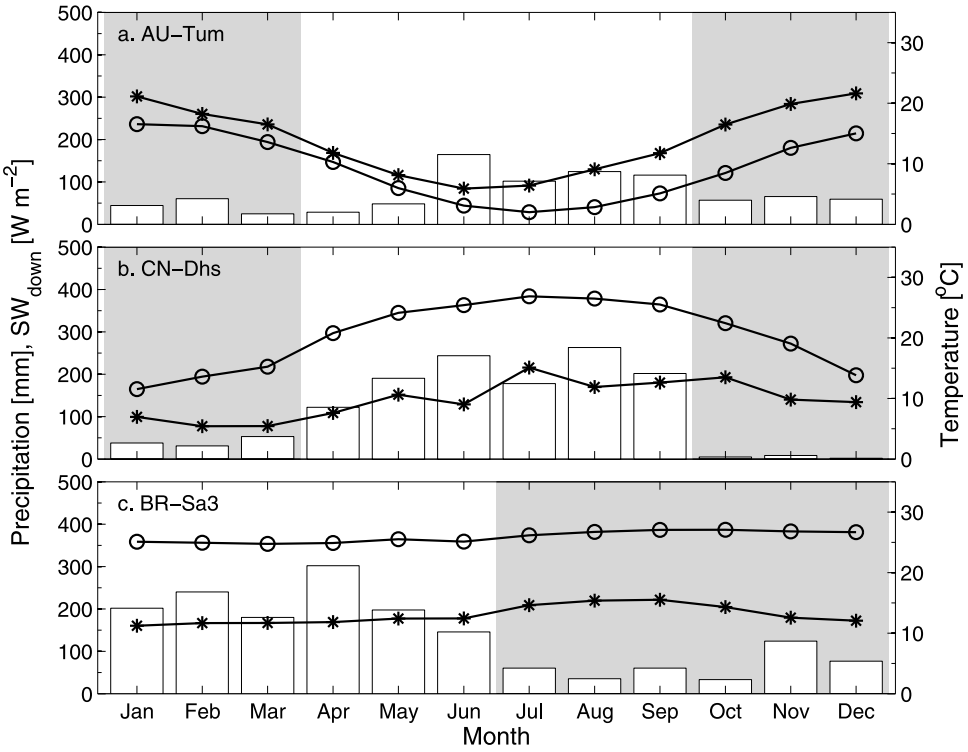

Figure 1. Monthly values of precipitation (bar), short wave downward radiation (SW_{down}, solid line with star) and temperature (solid line with circle) at the three sites: (a) Tumbarumba (AU-Tum) in Australia, (b) Dinghushan (CN-Dhs) in China, and (c) Tapajos National Forest (BR-Sa3) in Brazil. Shaded area indicates dry season.

[30] R is calculated as:

$$R = \frac{\sum_{j=1}^{N}(O-\bar{O})(P-\bar{P})}{\sqrt{\sum_{j=1}^{N}(O-\bar{O})^2\sum_{j=1}^{N}(P-\bar{P})^2}}. \quad (17)$$

The agreement index provides an overall assessment between model simulations and observations, and RMSE provides an estimate of the absolute bias in the model simulation; and complements R, the model simulations agree perfectly with observations only when RMSE = 0 and R = 1. The linear regression coefficients, the slope (b_s) and the intercept (b_0) are also used to justify the model's performance.

3. Results

[31] Incoming shortwave radiation, rainfall and air temperature are three major environmental drivers of NEE and Q_{LE}, which vary seasonally (see Figure 1). Mean annual rainfall over the study period was highest at CN-Dhs, about twice as much as that at AU-Tum. All three sites have a distinct dry and wet season. The dry season is warmer than the wet season at AU-Tum, but cooler at CN-Dhs. The seasonal variation of monthly air temperature is quite small (<2°C) at the BR-Sa3 site. These differences in the three major environmental drivers have resulted in significantly different local climates and hence responses of NEE and Q_{LE} to seasonal drought. All three sites are considered to be evergreen broadleaf forests in CABLE and therefore have the same parameter values unless specified otherwise. In situ observations from these three sites provide a good test of whether the alternative root water uptake function and hydraulic redistribution have similar effects on the CABLE simulations.

[32] In this study we compared the simulated responses of NEE and Q_{LE} of three evergreen broadleaf forests to seasonal drought using CABLE with four different configurations (see Table 2). Figure 2 shows the mean diurnal fluxes of Q_{LE} and NEE for wet (April) and dry (October) months at the BR-Sa3 site, where the difference between monthly precipitation in the wet and dry seasons is largest (302 mm in April versus 33 mm in October) among the three sites. The four simulations, S1–S4, did not differ from each other during wet season and the model agreed well with observations for both Q_{LE} and NEE (Figures 2a and 2c). During dry season, S1–S3 obviously underestimated daytime Q_{LE} by a large fraction (typically over 50% around noon time) and significantly underestimated the rate of carbon uptake during daytime. In contrast, S4 performed well and produced the closest agreement to the observations among the four simulations. Moreover, only S4 was able to reproduce the large amplitudes and the peak values of the observed fluxes of both Q_{LE} and NEE.

[33] At seasonal scales, simulation S4 reproduced the observed seasonal patterns of NEE and Q_{LE} (Figure 3) best among all four simulations. At the AU-Tum site, the seasonal pattern of NEE was captured well by S4. S1 to S3 predicted much more carbon release than was observed during the dry season. During the wet season, differences

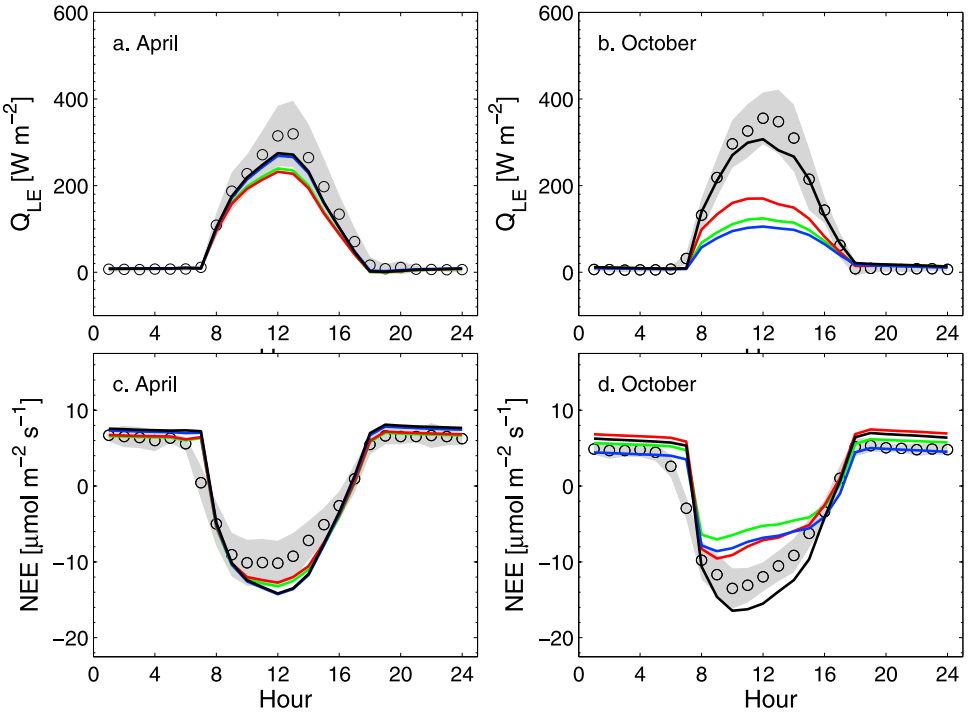

Figure 2. Difference among the simulated mean diurnal values of net ecosystem exchange (NEE) and latent heat flux (Q_{LE}) during (a, c) wet (April) and (b, d) dry (October) months at the BR-Sa3 site with four model smulations: S1 (green), S2 (red), S3 (blue), and S4 (black). The circle represents the observed values, and the shaded area represents ±1 standard deviation about the mean. Model simulations S1–S4 are defined in Table 2.

among four simulations S1–S4 were small and all agreed well with observed NEE (Figure 3a). Similarly, all simulations S1–S4 reproduced Q_{LE} reasonably well during wet seasons, but S1–S3 underestimated Q_{LE} during dry seasons. However, that underestimation was significantly reduced in S4 (Figure 3b). At the CN-Dhs site, differences in the simulated NEE or Q_{LE} were small among the four simulations, and all agreed well with observations (Figures 3c and 3d). At the BR-Sa3 site where variation of monthly precipitation within a year was largest among the three sites, the performance of four different model simulation was similar and the differences in the simulated mean daily NEE and Q_{LE} were small among all four simulations during the wet season, but were larger in the simulated daily NEE or Q_{LE} during the dry season. Only S4 reproduced the seasonal patterns of NEE and Q_{LE} at the BR-Sa3 site well, while simulations S1–S3 significantly overestimated daily NEE and underestimates Q_{LE} during dry season at this site (Figure 3f).

[34] Figure 4 shows that while there was reasonably good agreement between observed and modeled monthly NEE and Q_{LE} by CABLE using the described soil and vegetation parameter values (S1) at the CN-Dhs site, there was only poor agreement at the other two sites. At the CN-Dhs site, there were very small differences between S1–S4. The main reason was that both solar radiation and temperature (Figure 1b) were relatively low during dry seasons and the CN-Dhs forests may not suffer significant water stress. Both S1 and S2 greatly overestimated the carbon efflux and underestimated Q_{LE} during the dry seasons at BR-Sa3. S1, S2, and S3 all predicted a rapid increase in the carbon emission and decrease in Q_{LE} at AU-Tum during the dry season. Including hydraulic redistribution alone (as in S2) in CABLE generally slightly reduced the biases in simulated NEE and Q_{LE} for both BR-Sa3 and AU-Tum, as compared with S1, but the biases in both fluxes still remain quite large (see Table 3). When the alternative function for simulating root water uptake, as developed by *Lai and Katul* [2000] was used, (S3), the simulated NEE and Q_{LE} agreed much better with the observational data at the BR-Sa3 site during the dry seasons, but even worse than S1 at the AU-Tum site.

[35] When both hydraulic redistribution and the root water uptake function by *Lai and Katul* [2000] were used in CABLE (S4), the agreement between the modeled and observed NEE and Q_{LE} was greatly improved and agreed with observed fluxes best among all four simulations. The improvement in three measures of model performance from S4 was generally better for Q_{LE} than for NEE, particularly at BR-Sa3, as supported by the highest values of R^2 and d and smallest RMSE (Table 3). Analysis of a linear regression between the modeled and observed fluxes showed that improved performance of simulation has resulted in the slope being much closer to 1 than other simulations and the effect on the intercept was not significant (see Table 3).

[36] Either hydraulic redistribution or root water uptake can strongly influence plant responses to seasonal droughts at the AU-Tum and BR-Sa3 sites, but why are both modifications necessary for best performance of model simulations? We compared the observed (in situ) changes in soil moisture with those simulated by CABLE at AU-Tum and BR-Sa3. As shown in Figure 5 for the AU-Tum site, all four

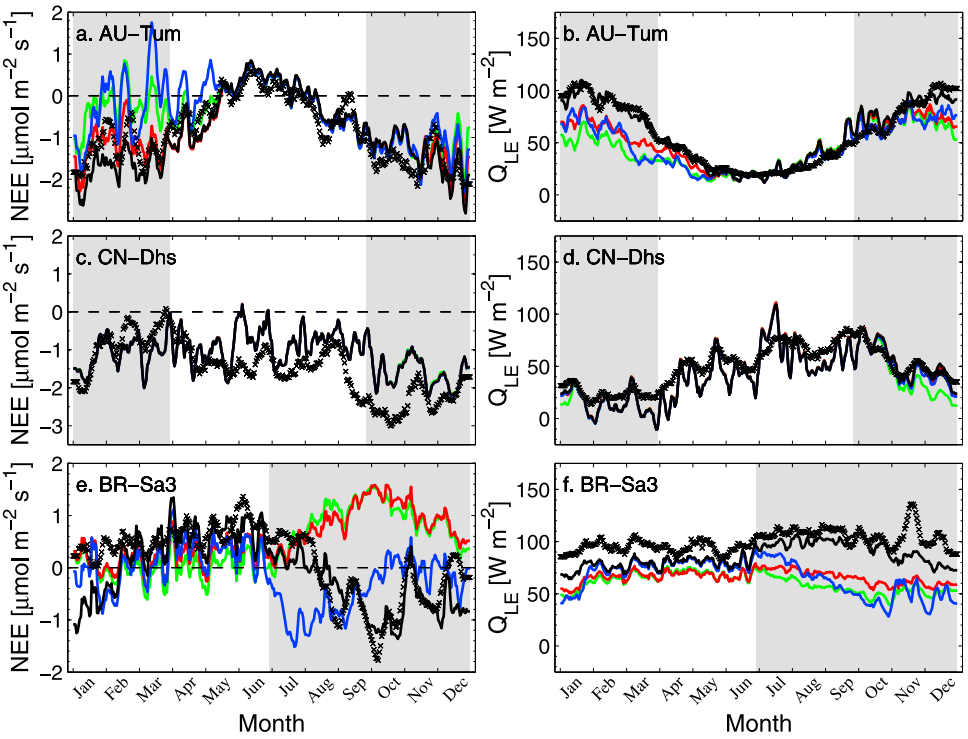

Figure 3. Difference among the simulated mean daily values of (left) NEE and (right) Q_{LE} over the year with four model simulations: S1 (green), S2 (red), S3 (blue), and S4 (black). The cross represents the observed values, and shaded areas represent the dry season. Model simulations S1–S4 are defined in Table 2.

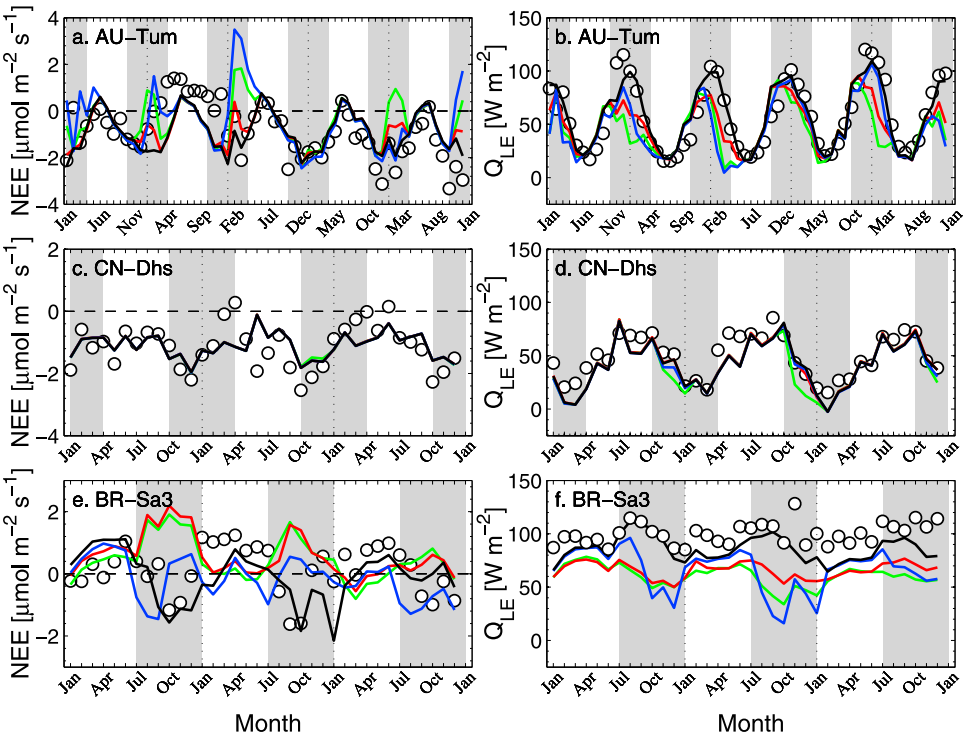

Figure 4. Comparison between measured (circle) monthly mean (left) NEE and (right) Q_{LE} at the three sites and the simulated values with four model simulations: S1 (green), S2 (red), S3 (blue), and S4 (black). Shaded area indicates dry season. The *x* axis is month of year.

Table 3. Flux Measurements at the Three Study Sites During Wet and Dry Seasons in Simulations S1–S4

		Wet Season				Dry Season			
Index	Site Code	S1	S2	S3	S4	S1	S2	S3	S4
				Net Ecosystem Exchange (NEE)					
d	AU-Tum	0.92	0.94	0.91	0.94	0.87	0.91	0.87	0.93
	CN-Dhs	0.87	0.87	0.87	0.87	0.90	0.90	0.90	0.90
	BR-Sa3	0.91	0.91	0.90	0.90	0.91	0.91	0.90	0.91
RMSE	AU-Tum	3.07	2.88	3.28	2.86	5.48	4.66	5.65	4.33
	CN-Dhs	4.01	4.01	4.01	4.01	2.96	2.93	2.93	2.93
	BR-Sa3	4.81	4.78	5.37	5.44	4.27	4.44	4.57	5.33
R^2	AU-Tum	0.79	0.81	0.75	0.81	0.68	0.77	0.65	0.79
	CN-Dhs	0.61	0.61	0.60	0.60	0.72	0.72	0.72	0.72
	BR-Sa3	0.72	0.72	0.70	0.72	0.70	0.72	0.67	0.77
b_s	AU-Tum	0.68	0.72	0.66	0.73	0.57	0.66	0.59	0.72
	CN-Dhs	0.65	0.65	0.65	0.65	0.63	0.64	0.64	0.64
	BR-Sa3	0.97	0.99	1.05	1.10	0.79	0.93	0.86	1.24
b_0	AU-Tum	0.02	−0.06	0.12	−0.03	0.05	−0.31	0.10	−0.53
	CN-Dhs	0.05	0.05	0.04	0.04	−0.33	−0.32	−0.33	−0.33
	BR-Sa3	−0.52	−0.33	−0.47	−0.35	1.13	1.19	−0.16	−0.06
				Latent Heat Transfer (Q_{LE})					
d	AU-Tum	0.84	0.87	0.84	0.89	0.77	0.84	0.83	0.92
	CN-Dhs	0.86	0.86	0.86	0.86	0.88	0.90	0.90	0.90
	BR-Sa3	0.84	0.85	0.87	0.89	0.72	0.80	0.75	0.91
RMSE	AU-Tum	39.63	36.39	38.72	35.31	90.91	76.19	81.68	60.49
	CN-Dhs	67.87	67.87	67.25	67.33	41.72	40.10	39.04	40.14
	BR-Sa3	85.58	83.70	82.62	76.82	110.87	98.05	111.42	76.74
R^2	AU-Tum	0.52	0.59	0.53	0.63	0.45	0.61	0.55	0.74
	CN-Dhs	0.57	0.57	0.57	0.57	0.62	0.68	0.67	0.68
	BR-Sa3	0.66	0.68	0.64	0.68	0.68	0.70	0.56	0.73
b_s	AU-Tum	0.69	0.75	0.68	0.83	0.46	0.55	0.55	0.74
	CN-Dhs	0.85	0.85	0.84	0.84	0.78	0.91	0.85	0.91
	BR-Sa3	0.53	0.54	0.60	0.65	0.36	0.45	0.39	0.67
b_0	AU-Tum	7.56	7.37	6.87	7.37	20.02	21.14	18.35	22.79
	CN-Dhs	−0.34	−0.37	−0.39	−0.45	−2.39	−1.38	−0.93	−1.21
	BR-Sa3	15.73	15.85	17.23	17.56	17.75	17.73	17.00	21.87

simulation (S1–S4) reproduced temporal variation of soil moisture reasonably well in the 15 cm soil, and only the two simulations with hydraulic redistribution (S2 and S4) performed better than the other two simulations (S1 and S3) in the soil layer between 15 cm and 30 cm deep. For two deeper soil layers, the CABLE simulation with Lai and Katul's root water uptake function (S3) performed better than other three simulations for soil moisture at a depth between 30 cm and 60 cm, but quite poor for the layer between 60 cm and 120 cm. Overall, S3 underestimated soil moisture but S4 overestimated for the two deep soil layers at AU-Tum site. At the BR-Sa3 site, the performance of four model simulations against the observed soil moisture varied with time and soil depth greatly (Figure 6). Overall S1 overestimated and S3 underestimated soil moisture at deep layers (between 120 cm to 350 cm), as compared with the observed.

[37] Differences in soil moisture content among different simulations can also be understood by comparing two different functions of root water extraction (see Figure 7). At any specific soil water content between wilting point and saturation, the value of η as calculated by the function of *Lai and Katul* [2000] was higher than that calculated by the default function in CABLE (Figure 7) when soil water content was low. During the dry seasons, deep soil layers were wetter than surface layers and their contribution to canopy transpiration as calculated using the function of *Lai and Katul* [2000] was larger than that using the default function in CABLE. As shown in Figure 5d and Figures 6d and 6e, the overestimation of deep soil moisture in S1 was much reduced in S3, and was further reduced when hydraulic redistribution was also included, as in S4.

[38] When the simulated seasonal variations of soil moisture at different depths were compared (see Figures 5 and 6), we found that the simulations with hydraulic redistribution (S2 and S4) generated much higher soil moisture content for the top 120 cm soil at AUS-Tum and the top 350 cm of soil at the BR-Sa3 site. Consequently the effect of reduced precipitation on NEE and Q_{LE} as simulated in S2 and S4 was much smaller than those in S1 and S3, respectively. Therefore hydraulic redistribution helped the ecosystem to remain physiolocally active throughout the dry season. Without hydraulic redistribution, CABLE is not able to capture correctly seasonal variations of NEE and Q_{LE} at both AUS-Tum and BR-Sa3 sites.

[39] Because NEE is the small difference between two large fluxes, gross primary production (GPP) and terrestrial ecosystem respiration (TER), a small error in either GPP or TER can result in large errors in NEE. While the differences in the simulated monthly NEE by all four simulations (S1–S4) were small at the CN-Dhs site, they are significant at the AUS-Tum and BR-Sa3 site, particularly during dry seasons. Figure 8a shows that the simulated GPP in S4 agreed most closely with the estimates from observations for all three sites, and the errors in the simulated NEE largely result from the errors in the simulated TER at the AU-Tum site. Neither hydraulic redistribution nor the alternative root

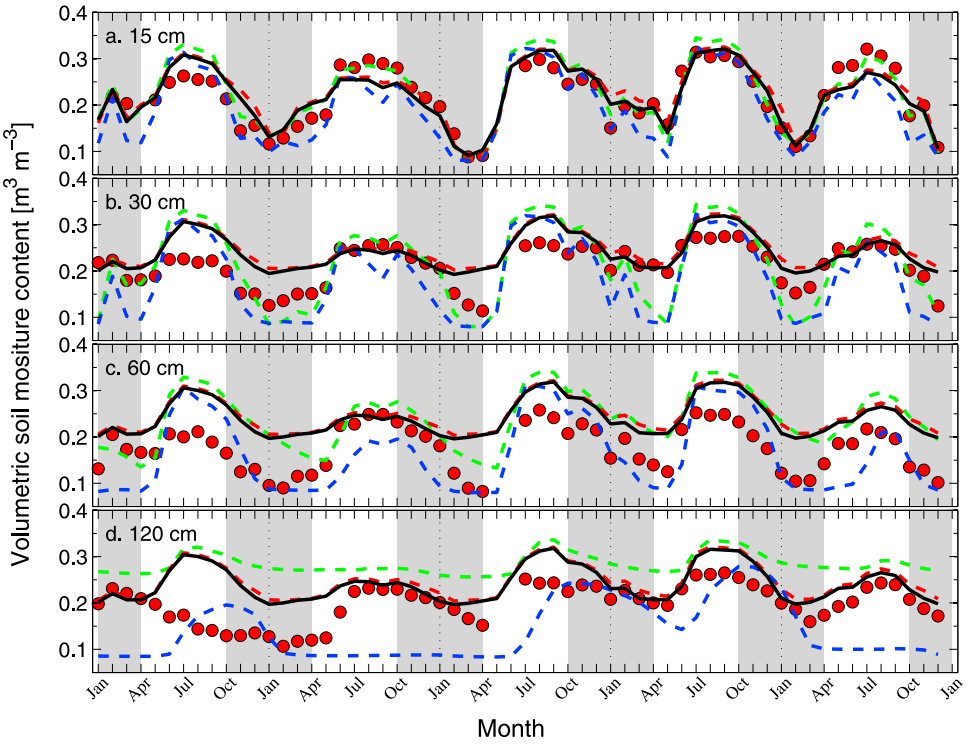

Figure 5. Comparison between monthly mean volumetric soil moisture ($m^3\ m^{-3}$) for each of four model simulations (S1 (green), S2 (red), S3 (blue), and S4 (black)) and the observed volumetric soil moisture content ($m^3\ m^{-3}$, filled circle) at the AU-Tum site. The *x* axis is month of year. Data for 2002–2006 are presented.

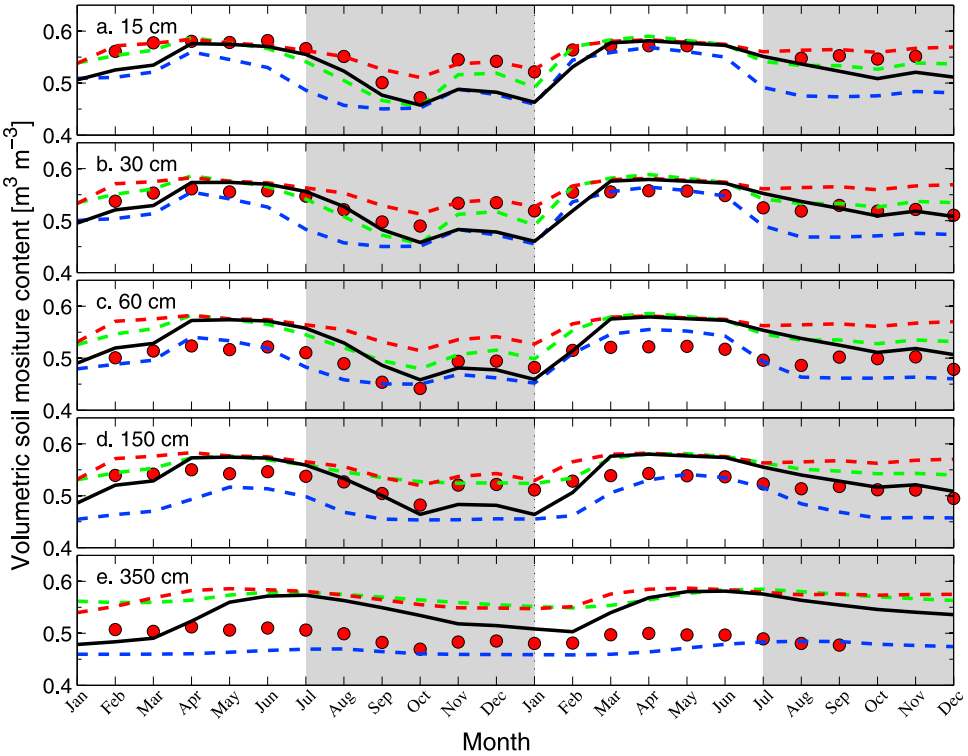

Figure 6. Comparison between monthly mean volumetric soil moisture ($m^3\ m^{-3}$) for each of four model simulations (S1 (green), S2 (red), S3 (blue), and S4 (black)) and the observed volumetric soil moisture content ($m^3\ m^{-3}$, filled circle) at the BR-Sa3 site. The *x* axis is month of year. Data for 2002–2003 are presented.

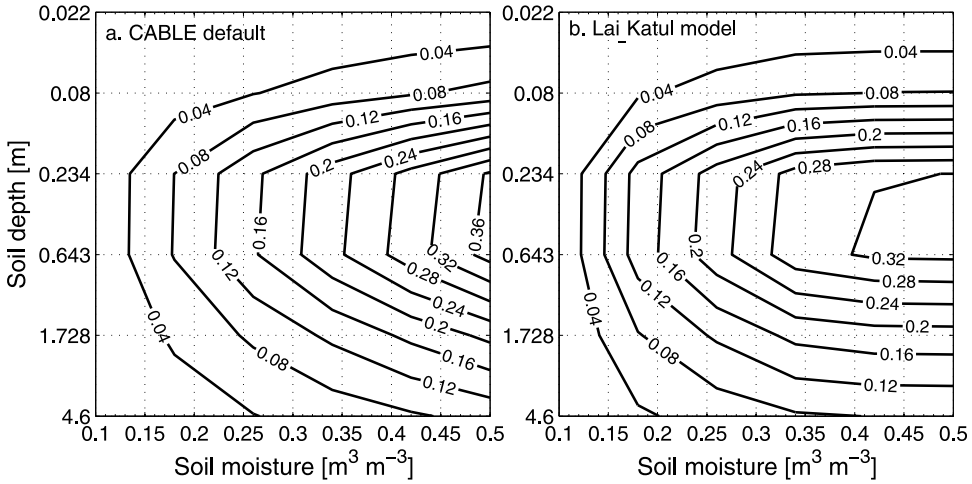

Figure 7. Value of η at different soil moisture contents as calculated using (a) the default function (equation (3)) or (b) the function developed by *Lai and Katul* [2000] (equation (4)). η was calculated with $\theta_{wilt} = 0.08$, $\theta_{sat} = 0.36$, and $\gamma = 0.01$. Same soil moisture content was assumed for all soil layers.

water uptake function significantly impacted simulated TER (see Figure 8b). CABLE simulations S1–S3 overestimated carbon release during the dry seasons at the AU-Tum site, largely as a result of underestimation of GPP by S1–S3. At CN-Dhs, the errors in simulated GPP and TER were relatively small, differences among four different simulations were also relatively small (<1 μmol m^{-2} s^{-1}) (Figures 8c and 8d). At the BR-Sa3 site, all simulations showed a decrease in TER from wet to dry seasons, but S4 agreed best with the measurements (Figure 8f). For GPP, only simulation S4 produced a small increase from wet to dry season. As a result, only simulation S4 predicted a larger carbon uptake during dry seasons than during wet season, which agreed well with the observed GPP (Figure 8e). The underlying reasons for a better agreement between S4 and the estimates of GPP from observations are related to the more efficient extraction of deep soil water by plants using the Lai and Katul's function than the default function in CABLE and

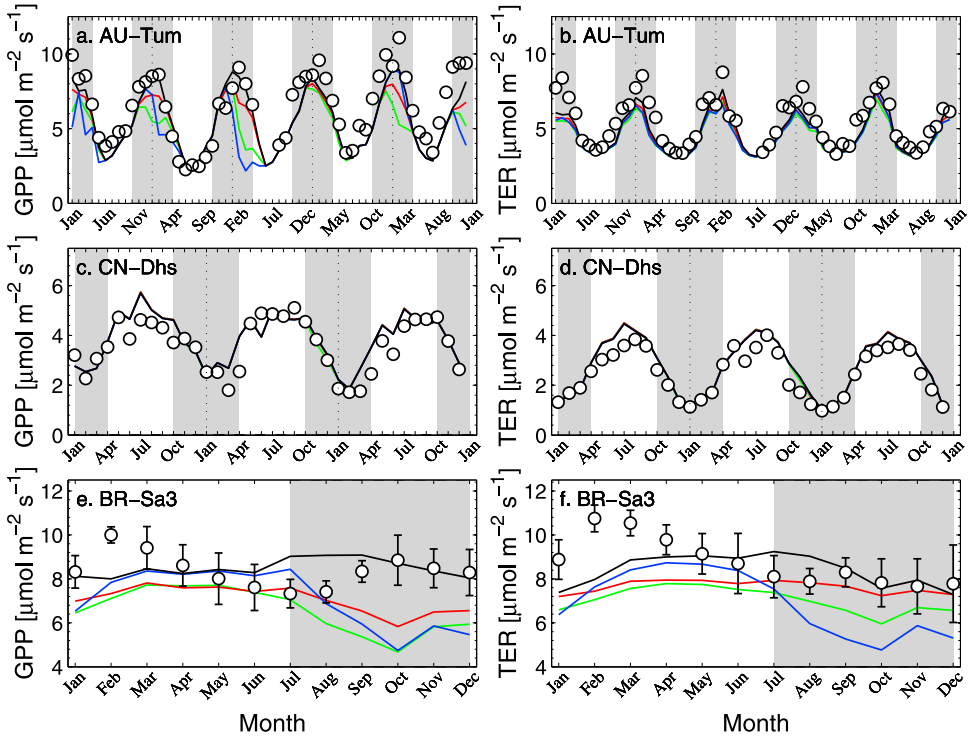

Figure 8. Comparison between the measured (circle) and simulated monthly mean (left) gross primary production (GPP) and (right) terrestrial ecosystem respiration (TER) at the three sites with four model simulations: S1 (green), S2 (red), S3 (blue), and S4 (black). Vertical bar in Figures 8e and 8f indicates error bar averaged for the three-year data. Shaded area indicates dry season. The *x* axis is month of year.

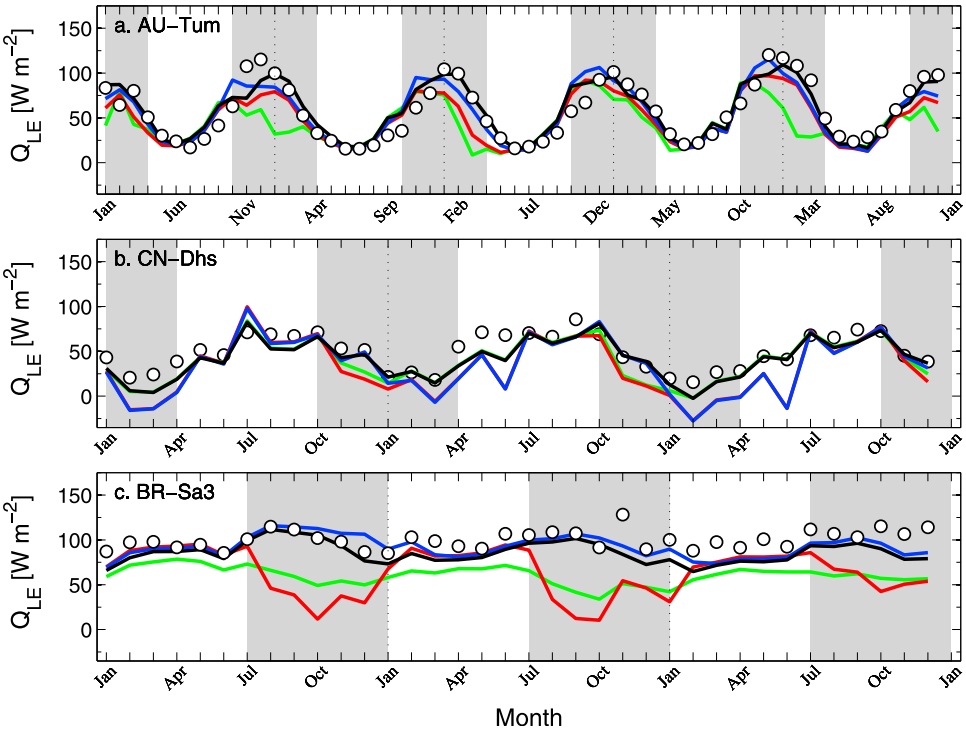

Figure 9. Comparison between the measured (circle) and the simulated Q_{LE} with the final simulation (S4 in Table 2, blue line), the default CABLE with described soil and vegetation parameters (S1, green line), the default CABLE (with all default soil and vegetation parameters from look-up tables; S17, red line), and S17 with Lai and Katul's root water uptake function and hydraulic redistribution (S18 in Table 2, black line). Shaded area indicates dry season. The *x* axis is month of year.

higher soil moisture as simulated by including hydraulic distribution (see Figure 6). As a result, simulation S4 correctly improved the simulated seasonal variations of Q_{LE}, GPP and TER, and better agreements with the observed NEE, as compared with other three model simulations.

[40] Values of some model parameters listed in Table 1 are site-specific, and are different from the default values as used in CABLE for global simulations. To assess how well CABLE will perform if default values from the parameter look-up tables [see *Kowalczyk et al.*, 2006] are used, two additional simulations (S17 and S18) were compared with the simulations with described soil and vegetation parameters S1 and S4 and the observed fluxes (see Figure 9). The results showed that the CABLE with all default soil and vegetation parameter values from look-up tables (S17) significantly underestimated Q_{LE} during the dry seasons at the BR-Sa3 site and some years at the Tum site, similar to that shown by S1. Simulation S17 differed slightly from S1, and the difference between them can be explained by the soil and vegetation parameters. Accounting for Lai and Katul's root water uptake function and hydraulic redistribution into S17 (S18) improved dry season Q_{LE}, and compared favorably with the observed Q_{LE} and the simulation S4 which was driven by more accurate site specific parameters.

4. Sensitivity Analysis

[41] As compared with S4, all model performance indices for more than 9 out of 12 simulations from S5 to S16 were relatively similar to S4. At the AU-Tum site, only the simulation with decreased value of υ by 25% (S8) caused a significant decrease in the model's performance, as measured by RMSE, R^2 and *d* index (Figure 10). Varying those six parameters with more than $\pm$25% or 10 times of their values had no significant effects on the three statistical indices at the CN-Dhs site. At the BR-Sa3 site, except for S8, increased γ and decreased K_{sat} by 10 times (S11 and S6, respectively) resulted in significant negative effects on the model's performance (Figure 10). The possible reason of the decreased model performance is that the parameters used in the S8, S11, and S6 simulation were out of the ranges of theirselves' reasonable values. These sensitive analysis results demonstrated that the improvement in model performance observed in S4 was not significantly affected by the values of the six parameters in CABLE, further justifying the significance of the two root functioning to the CABLE model.

5. Discussion

[42] In this study, we tested the effects of an alternative functional description of root water uptake and a hydraulic redistribution function in CABLE on the modeled responses of NEE and Q_{LE} to seasonality of rainfall at three evergreen broadleaf forests. The alternative function of root water uptake allows roots to extract water more efficiently per unit root mass in the deep and moist soil; the hydraulic redistribution function moves water passively through roots from the deep moist soil to dry surface soil layers for subsequent root uptake during the dry seasons. The agreement between the simulated NEE and Q_{LE} and observations at diurnal or

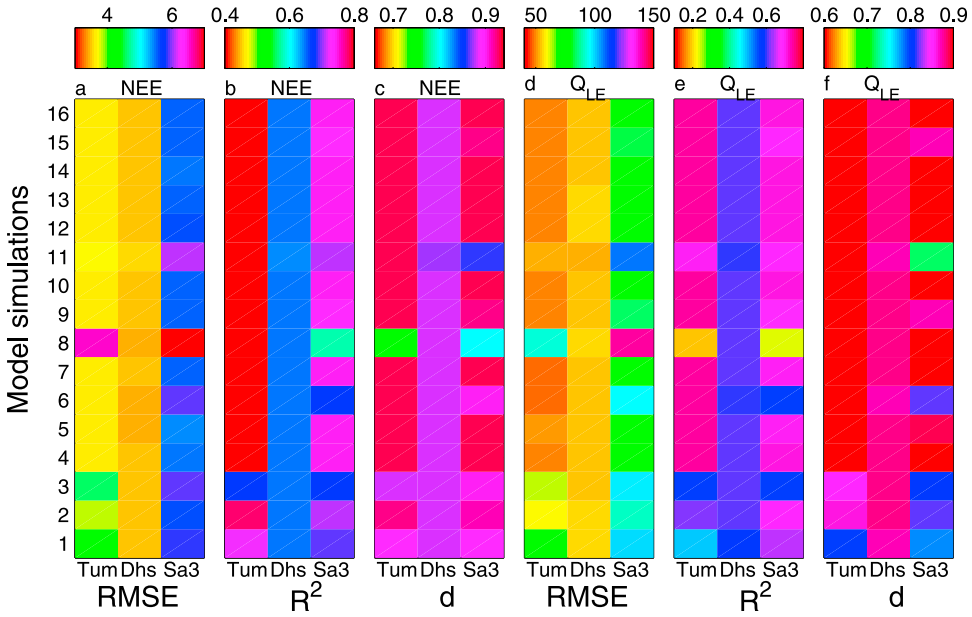

Figure 10. Sensitivities of the CABLE simulated hourly NEE and Q_{LE} to several and principle hydrological parameters (listed in Table 2) at the three sites. Shown are RMSE, R^2 and d index for all data combined. The units of RMSE are μmol m^{-2} s^{-1} and W s^{-1} for NEE and Q_{LE}, respectively. Model simulations S1–S16 are defined in Table 2.

seasonal scales were similar and good for all four simulation with or without these two root functions during the wet season. This suggests that modifying the model's root water uptake function and (or) incorporating hydraulic redistribution into the model does not impact the model's performance when soil moisture is readily available during the wet season. Most biases in the simulated NEE during the wet season at all three sites result from errors in the simulated ecosystem respiration by CABLE, as also found for other land surface models [*Baker et al.*, 2008; *Li et al.*, 2011]. During dry seasons, however, the performances of the default CABLE and the other two configurations with either modification of an alternative root water uptake function or a hydraulic redistribution function were much poorer than the simulations including both revised root functions (as in S4). This is supported by a number model performance measures used in this study.

[43] We have further demonstrated here why both mechanisms (efficient water uptake at depth and hydraulic redistribution) were needed in CABLE in order to reproduce the observed seasonal changes in NEE and Q_{LE} from wet to dry seasons at two of the three sites. At the CN-Dhs site, we found that the estimated water deficit (approximately defined as the difference between monthly rainfall and actual evapotranspiration) was minimal during the study (see Figure 11b), and the differences in the simulated NEE or Q_{LE} were relatively small among different simulations (S1 to S4), except for Q_{LE} during the dry seasons when the simulated Q_{LE} by S4 agreed slightly better than the other three simulations with the observed flux values (see Figure 4d). We calculated the contribution to modeled Q_{LE} from hydraulic redistribution and alternative root water uptake function as the difference in the simulated Q_{LE} between simulations S4 and S1, and found that that contribution was as high as over 70 mm per month during the dry seasons at AU-Tum and BR-Sa3, and was significantly and negatively correlated with the calculated water deficit at the two sites (see Figure 11). Over the study period, we estimated that the contributions to annual Q_{LE} were 23%, 3%, and 21% from hydraulic redistribution alone, or 27% (or 189 mm yr^{-1}), 6% (or 33 mm yr^{-1}), and 26% (or 315 mm yr^{-1}) when both hydraulic redistribution and alternative root water uptake was included during the study period at AU-Tum, CN-Dhs and BR-Sa3, respectively. These estimates agree well with the estimated contribution of 19% to 40% from previous studies for other ecosystems [see *Dawson*, 1996; *Ryel et al.*, 2002]. However, it has recently been argued that this estimate (19%–40%) contributed by deep roots may be an overestimate, in agreement with our findings of a 3%–27% contribution [see *Markewitz et al.*, 2010; *Neumann and Cardon*, 2012].

[44] Comparison of the annual totals for NEE, Q_{LE}, GPP and TER between observations and different CABLE simulations show that the overall agreement with the estimated fluxes from eddy flux towers is best for S4 at all three sites, especially for evapotranspiration (Figure 12).

[45] As shown in *Saleska et al.* [2003], many global models simulate the Amazonian tropical forests as being a carbon sink during the wet season and a carbon source during the dry season, contrary to field observations. As shown by *Baker et al.* [2008] using SiB3, a combination of several mechanisms including the two we applied here, is required to correctly represent the response of carbon fluxes to seasonal drought at the BR-Sa3 site. For the sake of numerical efficiency, and in contrast to the simulations of *Baker et al.* [2008], we did not extend our rooting depths in CABLE to 10 m soil, as that will involve substantial change of model code structure, and retained the default soil depth in CABLE of 4.6 m. The contribution to total canopy transpiration of soil water stored below 4.6 m may be significant [*Nepstad*

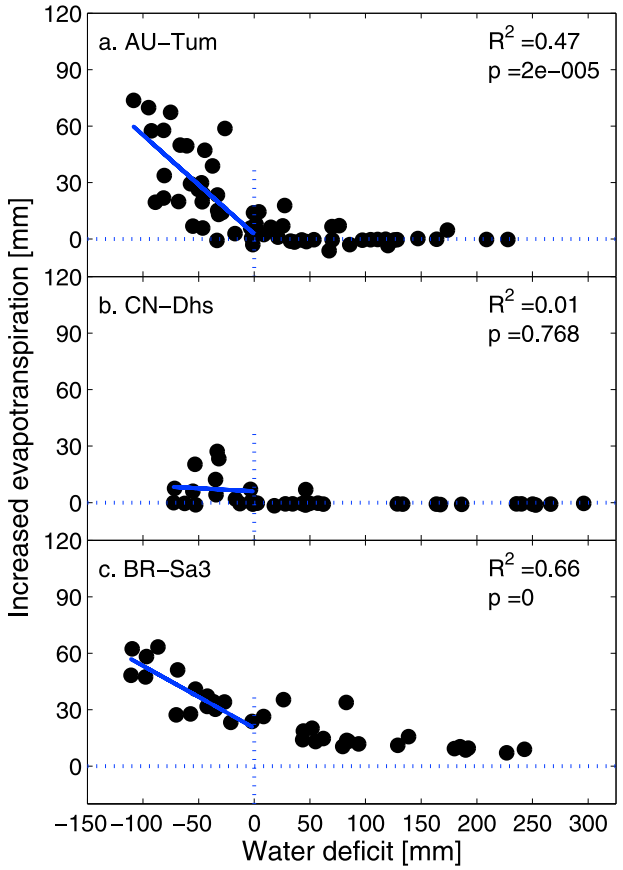

Figure 11. Relationship between water deficit (approximately defined as the difference between monthly rainfall and actual evapotranspiration) and increased evapotranspiration by integrating both hydraulic redistribution and alternative root water uptake function. R^2 and p are the square of linear correlation and p-value of significance between increased evapotranspiration and water deficit when water deficit values are negative.

et al., 1994; *Cook et al.*, 1998; *Davidson et al.*, 2011], but needs to be explored further.

[46] By analyzing the sensitivity of model performance to different values of six key model parameters, we showed that the improvement on model simulation performance at two of the three sites from including two root functions into CABLE was largely independent of the values of those six model parameter within reasonable ranges. Therefore same parameters values for the two root functions can be applied in CABLE to all three sites from temperate, subtropical and tropical climate conditions. This is further supported by the improvement in the CABLE performance when the two root functions were used in CABLE with values of all model parameters being set to their default values. These results from this study strongly encourage us to implement the two root functions into CABLE for further evaluation in the future.

[47] Land surface models have been often used for ecological and climatic research. Recent studies found that the predictions of carbon uptake by the terrestrial biosphere toward the end of this century by 11 different models differ widely, varying being a source of 6 Pg C $year^{-1}$ to a sink of 11 Pg C $year^{-1}$ by 2100 [see *Friedlingstein et al.*, 2006], and the regional differences in the predicted terrestrial carbon uptake are often largest in the tropics among those 11 models [see *Wang and Houlton*, 2009]. If those models cannot simulate observed seasonal variations of NEE or Q_{LE} under present climate conditions, their predictions for the future climate are likely to be unreliable. Plants can adapt to seasonally dry climates by developing deep roots, increasing the water uptake efficiency of deep roots and through hydraulic redistribution, and all of these processes have been well documented for many tree species [*Lai and Katul*, 2000; *Caldwell et al.*, 1998; *Burgess et al.*, 1998, 2001]. However, these processes have yet to be implemented into most global LSMs. This study shows that these root functions are required for accurately simulating the responses of carbon and water fluxes of evergreen broadleaf forests to seasonal drought under present or future climate conditions.

6. Conclusions

[48] The following conclusions can be drawn from this study:

[49] (1) The alternative function for root water uptake will allow roots in deep soil to take up water more efficiently per unit root mass, and hydraulic redistribution will move water passively via roots from deep moist soil to dry surface soil for subsequent uptake. Both mechanisms are needed in CABLE for simulating the seasonal responses of NEE and Q_{LE} to drought at two of the three forests;

[50] (2) The effects of those two mechanisms on the modeled responses to seasonal drought are not significantly affected by the values of other model parameters influencing

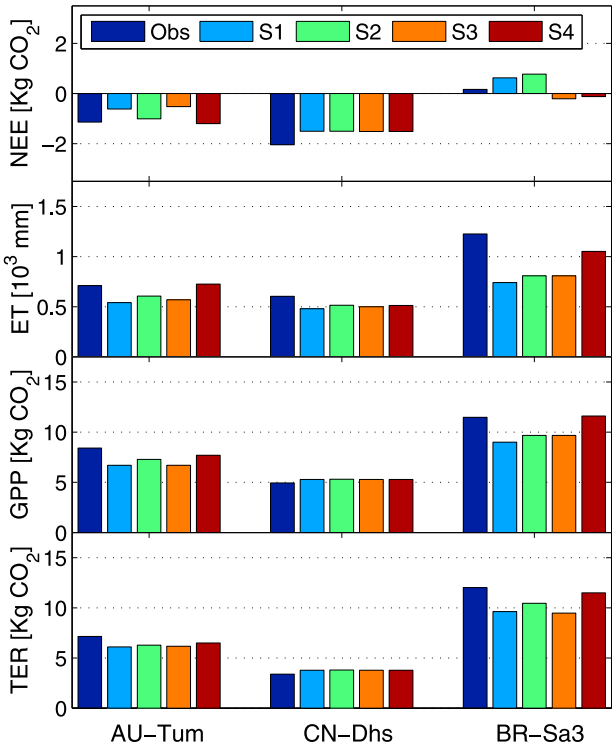

Figure 12. Comparisons of annual flux variables between observations and four simulations. ET is evapotranspiration; simulations S1–S4 are defined in Table 2.

soil water dynamics in those three forests. Therefore both mechanisms can be implemented into CABLE for regional or global studies of carbon and water dynamics.

[51] **Acknowledgments.** L. Li's research was supported in part by an Australian Research Council Discovery Early Career Research Award (DE120103022). The authors are grateful to Mike Goulden, Scott Miller, and Humberto da Rocha for providing the data for the BR-Sa3 site.

References

Abramowitz, G. (2005), Towards a benchmark for land surface models, *Geophys. Res. Lett.*, *32*, L22702, doi:10.1029/2005GL024419.

Abramowitz, G., A. Pitman, H. Gupta, E. Kowalczyk, and Y. P. Wang (2007), Systematic bias in land surface models, *J. Hydrometeorol.*, *8*, 989–1001, doi:10.1175/JHM628.1.

Araújo, A. C., et al. (2002), Comparative measurements of carbon dioxide fluxes from two nearby towers in a central Amazonian rainforests: The Manaus LBA site, *J. Geophys. Res.*, *107*(D20), 8090, doi:10.1029/2001JD000676.

Baker, I. T., L. Prihodko, A. S. Denning, M. Goulden, S. Miller, and H. R. da Rocha (2008), Seasonal drought stress in the Amazon: Reconciling models and observations, *J. Geophys. Res.*, *113*, G00B01, doi:10.1029/2007JG000644.

Bleby, T. M., A. J. Mcelrone, and R. B. Jackson (2010), Water uptake and hydraulic redistribution across large woody root systems to 20 m depth, *Plant Cell Environ.*, *33*, 2132–2148, doi:10.1111/j.1365-3040.2010.02212.x.

Bonan, G. B., P. J. Lawrence, K. W. Oleson, S. Levis, M. Jung, M. Reichstein, D. M. Lawrence, and S. C. Swenson (2011), Improving canopy processes in the Community Land Model version 4(CLM 4) using global flux fields empirically inferred from FLUXNET data, *J. Geophys. Res.*, *116*, G02014, doi:10.1029/2010JG001593.

Burgess, S. S. O., M. A. Adams, N. C. Turner, and C. K. Ong (1998), The redistribution of soil water by tree root systems, *Oecologia*, *115*, 306–311, doi:10.1007/s004420050521.

Burgess, S. S. O., M. A. Adams, N. C. Turner, C. R. Beverly, C. K. Ong, A. A. H. Khan, and T. M. Bleby (2001), An improved heat pulse method to measure low and reverse rates of sap flow in woody plants, *Tree Physiol.*, *21*, 589–598, doi:10.1093/treephys/21.9.589.

Caldwell, M. M., T. E. Dawson, and J. H. Richards (1998), Hydraulic lift: Consequences of water flux from the roots of plants, *Oecologia*, *113*, 151–161, doi:10.1007/s004420050363.

Canadell, J., R. B. Jackson, J. R. Ehleringer, H. A. Mooney, O. E. Sala, and E. D. Schulze (1996), Maximum rooting depth of vegetation types at the global scale, *Oecologia*, *108*, 583–595, doi:10.1007/BF00329030.

Carswell, F. E., A. L. Costa, M. Pahleta, Y. Malhi, P. Meir, J. P. R. Costa, M. L. Ruivo, L. S. M. Leal, R. Clement, and J. Grace (2002), Seasonality in CO_2 and H_2O flux at an eastern Amazonian rain forest, *J. Geophys. Res.*, *107*(D20), 8076, doi:10.1029/2000JD000284.

Cook, K. H., and E. K. Vizy (2008), Effects of twenty-first-century climate change on the Amazon rain forest, *J. Clim.*, *21*, 542–560, doi:10.1175/2007JCLI1838.1.

Cook, P. G., T. J. Hatton, D. Pidsley, A. L. Herczeg, A. Held, A. O'Grady, and D. Eamus (1998), Water balance of a tropical woodland ecosystem, northern Australia: A combination of micro-meteorological, soil physical and groundwater chemical approaches, *J. Hydrol.*, *210*, 161–177, doi:10.1016/S0022-1694(98)00181-4.

Cowan, I. R. (1965), Transport of water in the soil-plant-atmosphere system, *J. Appl. Ecol.*, *2*, 221–239, doi:10.2307/2401706.

Cruz, F. T., A. J. Pitman, and Y. P. Wang (2010), Can the stomatal response to higher atmospheric carbon dioxide explain the unusual temperatures during the 2002 Murray-Darling Basin drought?, *J. Geophys. Res.*, *115*, D02101, doi:10.1029/2009JD012767.

Dai, Y. J., et al. (2003), The Common Land Model (CLM), *Bull. Am. Meteorol. Soc.*, *84*, 1013–1023, doi:10.1175/BAMS-84-8-1013.

Davidson, E. A., P. A. Lefebvre, P. M. Brando, D. Ray, S. E. Trumbore, L. A. Solorzano, J. N. Ferreira, M. M. C. Bustamante, and D. C. Nepstad (2011), Carbon inputs and water uptake in deep soils of an eastern Amazon forest, *For. Sci. [Washington D. C.]*, *57*, 51–58.

Dawson, T. E. (1996), Determining water use by trees and forests from isotopic, energy balance and transpiration analyses: The roles of tree size and hydraulic lift, *Tree Physiol.*, *16*, 263–272, doi:10.1093/treephys/16.1-2.263.

Denning, A. S., G. J. Collatz, C. Zhang, D. A. Randall, J. A. Berry, P. J. Sellers, G. D. Colello, and D. A. Dazlich (1996), Simulations of terrestrial carbon metabolism and atmospheric CO_2 in a general circulation model. Part 1: Surface carbon fluxes, *Tellus, Ser. B*, *48*, 521–542, doi:10.1034/j.1600-0889.1996.t01-2-00009.x.

Eamus, D., and L. D. Prior (2001), Ecophysiology of trees of seasonally dry tropics: Comparisons among phenologies, *Adv. Ecol. Res*, *32*, 113–197, doi:10.1016/S0065-2504(01)32012-3.

Feddes, R. A., et al. (2001), Modeling root water uptake in hydrological and climate models, *Bull. Am. Meteorol. Soc.*, *82*, 2797–2809, doi:10.1175/1520-0477(2001)082<2797:MRWUIH>2.3.CO;2.

Friedlingstein, P., et al. (2006), Climate–carbon cycle feedback analysis: Results from the C4MIP model intercomparison, *J. Clim.*, *19*, 3337–3353, doi:10.1175/JCLI3800.1.

Goulden, M. L., S. D. Miller, H. R. da Rocha, M. C. Menton, H. C. de Freitas, A. M. E. S. Figueira, and C. A. S. de Sousa (2004), Diel and seasonal patterns of tropical forest CO_2 exchange, *Ecol. Appl.*, *14*, 42–54, doi:10.1890/02-6008.

Huntingford, C., et al. (2008), Towards quantifying uncertainty in predictions of Amazon 'dieback', *Philos. Trans. R. Soc. B*, *363*, 1857–1864, doi:10.1098/rstb.2007.0028.

Jackson, R. B., J. Canadell, J. R. Ehleringer, H. A. Mooney, O. E. Sala, and E. D. Schulze (1996), A global analysis of root distribution for terrestrial biomes, *Oecologia*, *108*, 389–411, doi:10.1007/BF00333714.

Jackson, R. B., J. S. Sperry, and T. E. Dawson (2000), Root water uptake and transport: Using physiological processes in global predictions, *Trends Plant Sci.*, *5*, 482–488, doi:10.1016/S1360-1385(00)01766-0.

Jarvis, P. G., and K. G. McNaughton (1986), Stomatal control of transpiration. Scaling up from leaf to region, *Adv. Ecol. Res*, *15*, 1–49, doi:10.1016/S0065-2504(08)60119-1.

Jones, C., J. Lowe, S. Liddicoat, and R. Betts (2009), Committed terrestrial ecosystem changes due to climate change, *Nat. Geosci.*, *2*, 484–487, doi:10.1038/ngeo555.

Keith, H., R. Leuning, K. L. Jacobsen, H. A. Cleugh, E. van Gorsel, R. J. Raison, B. E. Medlyn, A. Winters, and C. Keitel (2009), Multiple measurements constrain estimates of net carbon exchange by a Eucalyptus forest, *Agric. For. Meteorol.*, *149*, 535–558, doi:10.1016/j.agrformet.2008.10.002.

Keith, H., E. van Gorsel, K. L. Jacobsen, and H. Cleugh (2011), Dynamics of carbon exchange in a *Eucalyptus* forest in response to interacting disturbance factors, *Agric. For. Meteorol.*, *153*, 67–81, doi:10.1016/j.agrformet.2011.07.019.

Kleidon, A., and M. Heimann (2000), Assessing the role of deep rotted vegetation in the climate system with model simulations: Mechanism, comparison to observations and implications for Amazonian deforestation, *Clim. Dyn.*, *16*, 183–199, doi:10.1007/s003820050012.

Kowalczyk, E. A., Y. P. Wang, R. M. Law, H. L. Davies, J. L. McGregor, and G. Abramowitz (2006), The CSIRO Atmosphere Biosphere Land Exchange (CABLE) model for use in climate models and as an offline model, *CSIRO Mar. Atmos. Res. Pap. 013*, 42 pp.

Krinner, G., N. Viovy, N. de Noblet-Ducoudré, N. Ogée, J. Polcher, P. Friedlingstein, P. Ciais, S. Sitch, and I. C. Prentice (2005), A dynamic global vegetation model for studies of the coupled atmosphere-biosphere system, *Global Biogeochem. Cycles*, *19*, GB1015, doi:10.1029/2003GB002199.

Lai, C. T., and G. Katul (2000), The dynamic role of root-water uptake in coupling potential to actual transpiration, *Adv. Water Resour.*, *23*, 427–439, doi:10.1016/S0309-1708(99)00023-8.

Lee, J. E., R. S. Oliveira, T. E. Dawson, and I. Fung (2005), Root functioning modifies seasonal climate, *Proc. Natl. Acad. Sci. U. S. A.*, *102*(49), 17,576–17,581, doi:10.1073/pnas.0508785102.

Li, L., et al. (2011), Importance of crop varieties and management practices: Evaluation of a process-based model for simulating CO_2 and H_2O fluxes at five European maize (*Zea mays* L.) sites, *Biogeosciences*, *8*, 1721–1736, doi:10.5194/bg-8-1721-2011.

Ludwig, F., T. E. Dawson, H. Kroon, F. Brendse, and H. H. T. Prins (2003), Hydraulic lift in Acacia tortilis trees on an east African savanna, *Oecologia*, *134*, 293–300.

Markewitz, D., S. Devine, E. A. Davidson, P. Brando, and D. D. Nepstad (2010), Soil moisture depletion under simulated drought in the Amazon: Impacts on deep root uptake, *New Phytol.*, *187*, 592–607, doi:10.1111/j.1469-8137.2010.03391.x.

McElrone, A. J., W. T. Pockman, J. Martínez-Vilalta, and R. B. Jackson (2004), Variation in xylem structure and function in stems and roots of trees to 20 m depth, *New Phytol.*, *163*, 507–517, doi:10.1111/j.1469-8137.2004.01127.x.

McKenzie, N. J. (2004), *Australian Soils and Landscapes: An Illustrated Compendium*, CSIRO, Aspendale, Victoria, Australia.

Miller, S. D., M. L. Goulden, M. C. Menton, H. R. da Rocha, H. C. de Freitas, A. M. E. S. Figueira, and C. A. D. de Sousa (2004), Biometric and micrometeorological measurements of tropical forest carbon balance, *Ecol. Appl.*, *14*, 114–126, doi:10.1890/02-6005.

Mintz, Y. (1984), The sensitivity of numerically simulated climates to land-surface boundary conditions, in *The Global Climate*, edited by

J. T. Houghton, pp. 79–105, Cambridge Univ. Press, Cambridge, U. K.

Negrón Juárez, R. I. N., H. R. da Rocha, A. M. S. Figueira, M. L. Goulden, and S. D. Miller (2009), An improved estimate of leaf area index based on the histogram analysis of hemispherical photographs, *Agric. For. Meteorol.*, *149*, 920–928, doi:10.1016/j.agrformet.2008.11.012.

Nepstad, D. C., et al. (1994), The role of deep roots in the hydrological and carbon cycles of Amazonian forests and pastures, *Nature*, *372*, 666–669, doi:10.1038/372666a0.

Neumann, R. B., and Z. G. Cardon (2012), The magnitude of hydraulic redistribution by plant roots: A review and synthesis of empirical and modelling studies, *New Phytol.*, *194*, 337–352, doi:10.1111/j.1469-8137.2012.04088.x.

Oleson, K. W., et al. (2004), Technical description of the Community Land Model (CLM), *Tech. Note NCAR/TN-461+STR*, 173 pp., Natl. Cent. for Atmos. Res., Boulder, Colo.

Oliveira, R. S., T. E. Dawson, S. S. O. Burgess, and D. C. Nepstad (2005), Hydraulic redistribution in three Amazonian trees, *Oecologia*, *145*, 354–363, doi:10.1007/s00442-005-0108-2.

Pate, J. S., W. D. Jeschke, and M. J. Aylward (1995), Hydraulic architecture and xylem structure of the dimorphic root systems of South-West Australian species of Proteaceae, *J. Exp. Bot.*, *46*(8), 907–915, doi:10.1093/jxb/46.8.907.

Pitman, A. J., F. Avila, G. Abramowitz, Y. P. Wang, S. J. Phipps, and N. Noble-Ducoudré (2011), Importance of background climate in determining impact of land cover change on regional climate, *Nature Clim. Change*, *1*, 472–475, doi:10.1038/nclimate1294.

Potter, C., C. R. Klooster, C. R. de Carvalho, V. B. Genovese, A. Torregrosa, J. Dungan, M. Bobo, and J. Coughlan (2001), Modeling seasonal and interannual variability in ecosystem carbon cycling for the Brazilian Amazon region, *J. Geophys. Res.*, *106*(D10), 10,423–10,446, doi:10.1029/2000JD900563.

Raich, J. W., E. B. Rastetter, J. M. Melilllo, D. W. Kicklighter, P. A. Steudler, B. J. Peterson, A. L. Grace, B. Moore III, and C. J. Vorosmarty (1991), Potential net primary productivity in South America: Application of global model, *Ecol. Appl.*, *1*(4), 399–429, doi:10.2307/1941899.

Reichstein, M., et al. (2005), On the separation of net ecosystem exchange into assimilation and ecosystem respiration: Review and improved algorithm, *Global Change Biol.*, *11*, 1424–1439, doi:10.1111/j.1365-2486.2005.001002.x.

Richards, J. H., and M. M. Caldwell (1987), Hydraulic lift: Substantial nocturnal water transport between soil layers by *Artemisia tridentate* roots, *Oecologia*, *73*, 486–489, doi:10.1007/BF00379405.

Ryel, R. J., M. M. Caldwell, C. K. Yoder, D. Or, and A. J. Leffler (2002), Hydraulic redistribution in a stand of *Artemisia tridentata*: Evaluation of benefits to transpiration assessed with a simulation model, *Oecologia*, *130*, 173–184.

Ryel, R. J., M. M. Caldwell, A. J. Leffler, and C. K. Yoder (2003), Rapid soil moisture recharge to depth by roots in a stand of Artemisia tridentate, *Ecology*, *84*, 757–764, doi:10.1890/0012-9658(2003)084[0757:RSMRTD]2.0.CO;2.

Saleska, S. R., et al. (2003), Carbon in Amazon forests: Unexpected seasonal fluxes and disturbance induced losses, *Science*, *302*, 1554–1557, doi:10.1126/science.1091165.

Saleska, S. R., K. Didan, A. R. Huete, and H. R. da Rocha (2007), Amazon forests green-up during 2005 drought, *Science*, *318*, 612, doi:10.1126/science.1146663.

Schaap, M. G., F. J. Leij, and M. T. van Genuchten (2001), ROSETTA: A computer program for estimating soil hydraulic parameters with hierarchical pedotransfer functions, *J. Hydrol.*, *251*, 163–176, doi:10.1016/S0022-1694(01)00466-8.

Sellers, P. J., et al. (1996), A revised land surface parameterization (SiB2) for atmospheric GCMs. Part I: Model formulation, *J. Clim.*, *9*, 676–705, doi:10.1175/1520-0442(1996)009<0676:ARLSPF>2.0.CO;2.

Shukla, J., and Y. Mintz (1982), Influence of land-surface evaporation on the earth's climate, *Science*, *215*, 1498–1501, doi:10.1126/science.215.4539.1498.

Tang, X. L., Y. P. Wang, G. Y. Zhou, D. Q. Zhang, S. Liu, S. Z. Liu, Q. M. Zhang, J. X. Liu, and J. H. Yan (2011), Different patterns of ecosystem carbon accumulation between a young and an old-growth subtropical forest in Southern China, *Plant Ecol.*, *212*, 1385–1395, doi:10.1007/s11258-011-9914-2.

Thompson, S. E., C. J. Harman, A. G. Konings, M. Sivapalan, A. Neal, and P. A. Troch (2011), Comparative hydrology across AmeriFlux sites: The variable roles of climates, vegetation, and groundwater, *Water Resour. Res.*, *47*, W00J07, doi:10.1029/2010WR009797.

Tuzet, A., A. Perrier, and R. Lening (2003), A coupled model of stomatal conductance, photosynthesis and transpiration, *Plant Cell Environ.*, *26*, 1097–1116, doi:10.1046/j.1365-3040.2003.01035.x.

van Genuchten, M. T. (1980), A closed-form equation for predicting the hydraulic conductivity of unsaturated soils, *Soil Sci. Soc. Am. J.*, *44*, 892–898, doi:10.2136/sssaj1980.03615995004400050002x.

van Gorsel, E., R. Leuning, H. Cleugh, H. Keith, and T. Suni (2007), Nocturnal carbon efflux: Reconciliation of eddy covariance and chamber measurements using an alternative to the u*-threshold filtering technique, *Tellus, Ser. B*, *59*(3), 397–403, doi:10.1111/j.1600-0889.2007.00252.x.

van Gorsel, E., R. Leuning, H. Cleugh, H. Keith, M. U. F. Kirschbaum, and T. Suni (2008), Application of an alternative method to derive reliable estimates of nighttime respiration from eddy covariance measurements in moderately complex topography, *Agric. For. Meteorol.*, *148*(6–7), 1174–1180, doi:10.1016/j.agrformet.2008.01.015.

van Gorsel, E., et al. (2009), Estimating nocturnal ecosystem respiration from the vertical turbulent flux and change in storage of CO_2, *Agric. For. Meteorol.*, *149*(11), 1919–1930, doi:10.1016/j.agrformet.2009.06.020.

Vourlitis, G. L., N. Priante, M. M. S. Hayashi, J. D. Nogueira, F. T. Caseiro, and J. H. Campelo (2001), Seasonal variantions in the net ecosystem CO_2 exchange of a mature Amazonian transitional tropical forest (cerradáo), *Funct. Ecol.*, *15*(3), 388–395, doi:10.1046/j.1365-2435.2001.00535.x.

Wang, C. L., G. R. Yu, G. Y. Zhou, J. H. Yan, L. M. Zhang, X. Wang, X. L. Tang, and X. M. Sun (2006), CO_2 flux evaluation over the evergreen coniferous and broad-leaved mixed forest in Dinghushan, China, *Science in China Series D, Earth Sci.*, *49*, 127–138.

Wang, Y.-P., and B. Z. Houlton (2009), Nitrogen constraints on terrestrial carbon uptake: Implications for the global carbon-climate feedback, *Geophys. Res. Lett.*, *36*, L24403, doi:10.1029/2009GL041009.

Wang, Y. P., R. Leuning, H. A. Cleugh, and P. A. Coppin (2001), Parameter estimation in surface exchange models using nonlinear inversion: How many parameters can we estimate and which measurements are most useful?, *Global Change Biol.*, *7*, 495–510, doi:10.1046/j.1365-2486.2001.00434.x.

Wang, Y. P., D. Baldocchi, R. Leuning, E. Falge, and T. Vesala (2007), Estimating parameters in a land surface model by applying nonlinear inversion to eddy covariance flux measurements from eight FLUXNET sites, *Global Change Biol.*, *13*, 652–670, doi:10.1111/j.1365-2486.2006.01225.x.

Wang, Y. P., R. M. Law, and B. Pak (2010), A global model of carbon, nitrogen and phosphorus cycles for the terrestrial biosphere, *Biogeosciences*, *7*, 2261–2282, doi:10.5194/bg-7-2261-2010.

Wang, Y.-P., E. Kowalczyk, R. Leuning, G. Abramowitz, M. R. Raupach, P. Bernard, E. van Gorsel, and A. Luhar (2011), Diagnosing errors in a land surface model (CABLE) in the time and frequency domains, *J. Geophys. Res.*, *116*, G01034, doi:10.1029/2010JG001385.

Willmott, C. J. (1981), On the validation of models, *Phys. Geogr.*, *2*(2), 184–194.

Yu, G. R., Y. L. Fu, X. M. Sun, X. F. Wen, and L. M. Zhang (2006), Recent progress and future directions of ChinaFLUX, *Sci. China, Ser. D*, *49*, 1–23, doi:10.1007/s11430-006-8001-3.

Zegelin, S. J., and I. White (1989), Improved field probes for soil water content and electrical conductivity measurement using time domain reflectometry, *Water Resour. Res.*, *25*, 2367–2376, doi:10.1029/WR025i011p02367.

Zhang, H. Q., L. Zhang, and B. Pak (2011), Comparing surface energy, water and carbon cycle in dry and wet regions simulated by a land surface model, *Theor. Appl. Climatol.*, *104*, 511–527, doi:10.1007/s00704-010-0364-x.

Zhang, M., et al. (2011), Effects of cloudiness change on net ecosystem exchange, light use efficiency, and water use efficiency in typical ecosystems of China, *Agric. For. Meteorol.*, *151*, 803–816, doi:10.1016/j.agrformet.2011.01.011.

Zheng, Z., and G. L. Wang (2007), Modeling the dynamic root water uptake and its hydrological impact at the Reserva Jaru site in Amazonia, *J. Geophys. Res.*, *112*, G04012, doi:10.1029/2007JG000413.